2023 62nd IEEE Conference on Decision and Control (CDC)
December 13-15, 2023. Marina Bay Sands, Singapore

Data-Enabled Neighboring Extremal Optimal Control: A Computationally Efficient DeePC

Amin Vahidi-Moghaddam, Kaixiang Zhang, Zhaojian Li and Yan Wang

Abstract— **Model-based optimal control strategies typically rely on accurate parametric representations of the underlying systems, which can be challenging to obtain, especially for nonlinear and complex systems. Therefore, data-driven optimal controllers have become increasingly attractive to both academics and industry practitioners. As a data-driven optimal control approach that can explicitly handle constraints, data-enabled predictive control (DeePC) makes a transition from the model-based optimal control strategies (e.g. model predictive control (MPC)) to a data-driven one such that it seeks an optimal control policy from raw input/output (I/O) data without requiring system identification prior to control deployment, achieving remarkable successes in various applications. However, this approach involves high computational cost due to the dimension of the decision variable, which is generally significantly higher than its MPC counterpart. Several approaches have been proposed to reduce the computational cost of the DeePC for linear time-invariant (LTI) systems. However, finding a computationally efficient method to implement the DeePC for the nonlinear systems is still an open challenge. In this paper, we propose a data-enabled neighboring extremal (DeeNE) to approximate the DeePC policy and reduce its computational cost for the constrained nonlinear systems. The DeeNE adapts a pre-computed nominal DeePC solution to the perturbations of the initial I/O trajectory and the reference trajectory from the nominal ones. We also develop a scheme to handle nominal non-optimal solutions so that we can use the DeeNE solution as the nominal solution during the control process. Promising simulation results on the cart inverted pendulum problem demonstrate the efficacy of the DeeNE framework.**

I. Introduction

As systems become increasingly complex and the data gets more accessible, scientists and practitioners are turning to data-driven methods instead of classical model-based techniques for system controls [1]. While model-based controllers rely on accurate plant modeling, data-driven control approaches synthesize a controller from input/output (I/O) data collected on the real system [2]–[5]. There are two paradigms of data-driven control: i) indirect data-driven control that first identifies a model using the I/O data and then conducts control design based on the identified model [6], [7], and ii) direct data-driven control that circumvents the step of system identification and obtains control policy directly from the I/O data [8]. A central promise is that the direct data-driven control may have higher flexibility and better performance than the indirect data-driven control thanks to the data-centric representation that avoids using a specific model from identification [9].

Recently, a result in the context of behavioral system theory [10], known as Fundamental Lemma [11], has received renewed attention in the direct data-driven control. Rather than attempting to learn a parametric system model, this result enables one to learn the system's behaviour such that the subspace of the I/O trajectories of a linear time invariant (LTI) system can be obtained from column span of a data Hankel matrix. A direct data-driven optimal control, called data-enabled predictive control (DeePC) [12], has recently been proposed in the spirit of the Fundamental Lemma. The DeePC algorithm relies only on the I/O data to learn the behavior of the unknown system and perform safe and optimal control to drive the system along a desired trajectory using real-time feedback. In comparison with the machine learning-based controllers, the DeePC is more computationally efficient, less data hungry, and more suitable to rigorous stability and robustness analysis [13]. The DeePC algorithm has been successfully applied in many scenarios, including quadcopters [14] and power systems [15].

Despite the promise, the DeePC generally suffers from high computation complexity because of the high dimension of the decision variables. To address this challenge, several approaches have been proposed to optimize a lower dimension decision variable and reduce the computational cost of the DeePC for the LTI systems. For example, subspace predictive control (SPC) [15], [16] identifies a reduced-order model for the linear DeePC using the singular value decomposition of the raw data; however, it is not a pure data-driven controller due to the identification part. Null-space predictive control (NPC) [13] introduces a lower dimension decision variable to reduce the computational cost of the DeePC, but it only works for the unconstrained linear DeePC. Minimum-dimension DeePC [17] uses the singular value decomposition to make more efficient numerical computation for the constrained linear DeePC. However, for the nonlinear systems, the computational cost of the DeePC is still a challenging problem and needs to be solved. It is worth noting that for the SPC and the minimum-dimension DeePC, the choice of the number of the singular values to retain/cut is very critical and nontrivial.

Considering the above challenges on the dimension-reduction techniques [17]–[19], neighboring extremal (NE) [20] is a promising paradigm to attain (sub-)optimal performance with efficient computations, which is suitable for the systems with fast dynamics and limited onboard compu-

This work was partially supported by the U.S. National Science Foundation Award CMMI-2320698.

Amin Vahidi-Moghaddam, Kaixiang Zhang, and Zhaojian Li are with the Department of Mechanical Engineering, Michigan State University, East Lansing, MI 48824 USA (e-mail: vahidimo@msu.edu, zhangk64@msu.edu, lizhaoj1@egr.msu.edu).

Yan Wang was with the Research and Advanced Engineering, Ford Motor Company, Dearborn, MI 48121 USA (e-mail: ucsb1997@gmail.com).

tations. Specifically, given a pre-computed nominal solution based on its nominal initial state, the NE provides an optimal correction law (to the first order) to the deviations from the computed nominal values [21], [22]. The nominal control law can be obtained from a remote powerful controller or can be computed ahead of time based on an approximated initial state. The resulting NE control law is a time-varying feedback gain on the state deviations that can be pre-computed along with the original optimal control problem. Therefore, this adaptation requires negligible online computation and can thus be used towards nonlinear optimal control problems that are computationally too expensive to solve at each time step. The NE has been employed in several engineering systems, including ship maneuvering control [23], power management [24], full bridge DC/DC converter [25], and spacecraft relative motion maneuvers [26]. However, existing NE frameworks only deal with model-based controllers while the data-driven controllers have extensively been employed in modern applications.

In this paper, we develop a data-enabled NE (DeeNE) framework for the nonlinear DeePC problem with initial I/O and reference perturbations to address the challenge of high computational cost in the DeePC.

II. Preliminaries and Problem Formulation

Consider the following discrete-time nonlinear system:

$$\begin{aligned} x(k+1) &= f(x(k), u(k)), \\ y(k) &= h(x(k), u(k)), \end{aligned} \tag{1}$$

where $k \in \mathbb{N}^+$ denotes the time step, $x \in \mathbb{R}^n$ represents the state vector of the system, $u \in \mathbb{R}^m$ is the control input, and $y \in \mathbb{R}^p$ denotes the outputs of the system. Moreover, $f : \mathbb{R}^n \times \mathbb{R}^m \to \mathbb{R}^n$ is the system dynamics with $f(0,0) = 0$, and $h : \mathbb{R}^n \times \mathbb{R}^m \to \mathbb{R}^p$ represents the output dynamics.

We consider the following safety constraint:

$$C(y(k), u(k)) \leq 0, \tag{2}$$

where $C : \mathbb{R}^p \times \mathbb{R}^m \to \mathbb{R}^l$. We consider the nonlinear system (1) and a tracking control problem with the desired trajectory $r(k)$. Starting from an initial state x_0, the closed-loop system performance over N steps is characterized by the following cost term:

$$J_N(\mathbf{y}, \mathbf{u}; \mathbf{r}) = \sum_{\mathbf{k=0}}^{\mathbf{N-1}} \phi(\mathbf{y(k)}, \mathbf{u(k)}; \mathbf{r(k)}), \tag{3}$$

where $\mathbf{u} = [u(0), u(1), \cdots, u(N-1)]$, $\mathbf{y} = [y(0), y(1), \cdots, y(N-1)]$, $\mathbf{r} = [r(0), r(1), \cdots, r(N-1)]$, and $\phi(y, u; r)$ is the stage cost.

The optimal control problem aims at optimizing the system performance over N future steps for (1), which is reduced to the following constrained optimization problem:

$$\begin{aligned} (\mathbf{y}^*, \mathbf{u}^*) = \arg\min_{\mathbf{y},\mathbf{u}} \ & J_N(\mathbf{y}, \mathbf{u}; \mathbf{r}) \\ s.t. \quad & x(k+1) = f(x(k), u(k)) \\ & y(k) = h(x(k), u(k)) \\ & C(y(k), u(k)) \leq 0. \end{aligned} \tag{4}$$

The model-based optimal control (4) is one of the most celebrated and widely used control techniques for trajectory tracking, due to its capability to enforce safety constraints during the control design. The key ingredient for this controller is an accurate parametric model of the system, but obtaining such a model, using plant modeling or identification procedures, is often the most time-consuming and cost part of control design.

Fundamental Lemma [11] inspires an alternative, non-parametric way to represent the system model (1). More specifically, Hankel matrices $\mathbb{H}(u^d)$ and $\mathbb{H}(y^d)$ are first constructed from the offline collected I/O samples u^d and y^d as

$$\mathbb{H}(u^d) = \begin{bmatrix} u_1 & u_2 & \cdots & u_{T-T_{ini}-N+1} \\ u_2 & u_3 & \cdots & u_{T-T_{ini}-N+2} \\ \vdots & \vdots & \ddots & \vdots \\ u_{T_{ini}+N} & u_{T_{ini}+N+1} & \cdots & u_T \end{bmatrix}, \tag{5}$$

and $\mathbb{H}(y^d) \in \mathbb{R}^{p(T_{ini}+N)\times L}$ is built in an analogous way from the collected samples y^d. $\mathbb{H}(u^d) \in \mathbb{R}^{m(T_{ini}+N)\times L}$ needs to have full row rank to satisfy the persistency of excitation requirement, and the number of its columns is denoted as $L = T - T_{ini} - N + 1$. Then, the Hankel matrices are partitioned in Past and Future subblocks:

$$\begin{bmatrix} U_P \\ U_F \end{bmatrix} =: \mathbb{H}(u^d), \qquad \begin{bmatrix} Y_P \\ Y_F \end{bmatrix} =: \mathbb{H}(y^d), \tag{6}$$

where $U_P \in \mathbb{R}^{mT_{ini}\times L}$, $U_F \in \mathbb{R}^{mN\times L}$, $Y_P \in \mathbb{R}^{pT_{ini}\times L}$, and $Y_F \in \mathbb{R}^{pN\times L}$.

The data-enabled predictive control (DeePC) is then formulated as a data-driven alternative of (4) as [12], [27]:

$$\begin{aligned} (\mathbf{y}^*, \mathbf{u}^*, \sigma_{\mathbf{y}}{}^*, \sigma_{\mathbf{u}}{}^*, \mathbf{g}^*) = & \arg\min_{\mathbf{y},\mathbf{u},\sigma_{\mathbf{y}},\sigma_{\mathbf{u}},\mathbf{g}} J_N(\mathbf{y}, \mathbf{u}, \sigma_{\mathbf{y}}, \sigma_{\mathbf{u}}, \mathbf{g}) \\ s.t. \quad & \begin{bmatrix} U_P \\ Y_P \\ U_F \\ Y_F \end{bmatrix} g = \begin{bmatrix} u_{ini} \\ y_{ini} \\ u \\ y \end{bmatrix} + \begin{bmatrix} \sigma_u \\ \sigma_y \\ 0 \\ 0 \end{bmatrix}, \qquad C(y,u) \leq 0, \end{aligned} \tag{7}$$

where the equality constraint is a result of the fundamental lemma with $\sigma_u \in \mathbb{R}^{mT_{ini}}$ and $\sigma_y \in \mathbb{R}^{pT_{ini}}$ being auxiliary slack variables to model measurement noises and nonlinearities, and $J_N(\mathbf{y}, \mathbf{u}, \sigma_{\mathbf{y}}, \sigma_{\mathbf{u}}, \mathbf{g})$ is the modified cost function for data-driven controllers with noisy data and nonlinearities [27]. Note that one can rewrite (7) as

$$\begin{aligned} \mathbf{g}^* = & \arg\min_{\mathbf{g}} J_N(Y_F\mathbf{g}, U_F\mathbf{g}, Y_P g - y_{ini}, U_P g - u_{ini}, g) \\ s.t. \quad & C(Y_F g, U_F g) \leq 0, \end{aligned} \tag{8}$$

using the identities $y = Y_F g$, $u = U_F g$, $\sigma_y = Y_P g - y_{ini}$, and $\sigma_u = U_P g - u_{ini}$ from (7).

If the constraint $C(y,u)$ is absent in (7), the problem is referred to the unconstrained DeePC, and the solution is available in closed form with reduced computational burden. For this case, one has $u = U_F g = K_d^r r + K_d^{ini} w_{ini}$ as the DeePC policy, where $K_d^r \in \mathbb{R}^{mN\times pN}$ and $K_d^{ini} \in \mathbb{R}^{mN\times(m+p)T_{ini}}$ are control gains, r is the desired reference trajectory, and $w_{ini} = \left[u_{ini}^T, y_{ini}^T\right]^T$ is the given initial trajectory. However, the constrained DeePC (7) suffers from high computational cost.

III. Main Result

In this section, given a nominal solution (g^o, u^o, y^o) (e.g., solved from (8)), we propose a data-enabled neighboring extremal (DeeNE) to efficiently adapt to small initial (I/O) and reference trajectories perturbations without the need of recomputing the optimal solution.

A. Nominal Lagrange Multipliers

Considering (8), the augmented cost function is constructed:

$$\bar{J}_N(w_{ini}, g, r, \mu) = J_N(w_{ini}, g, r) + \mu^T C^a(w_{ini}, g), \tag{9}$$

where $C^a(w_{ini}, g)$ represents the active constraints, and μ is the Lagrange multiplier associated with the active constraints. Let (w^o_{ini}, g^o, r^o) represent the nominal solution to the DeePC (7), which must satisfy the following KKT necessary optimality conditions:

$$\bar{J}_g(w_{ini}, g, r, \mu) = 0, \qquad \mu \geq 0, \tag{10}$$

where $\bar{J}_g$ indicates $\partial \bar{J}_N / \partial g$.

Assumption 1. *$C^a_g(w_{ini}, g)$ is full row rank.*

Substituting the nominal solution (w^o_{ini}, g^o, r^o) into the above KKT conditions and from (10), it follows that

$$J_g(w^o_{ini}, g^o, r^o) + \mu^T C^a_g(w^o_{ini}, g^o) = 0. \tag{11}$$

The Lagrange multiplier can thus be obtained online as:

$$\mu = -(C^a_g C^{aT}_g)^{-1} C^a_g J^T_g. \tag{12}$$

Note that Assumption 1 guarantees that $C^a_g C^{aT}_g$ is invertible. Moreover, it is worth noting that $\mu = 0$ if the constraint $C(w^o_{ini}, g^o)$ is not active. The Lagrange multiplier (12) is considered as the nominal optimal Lagrange multiplier μ^o.

B. Data-Enabled Neighboring Extremal (DeeNE)

Consider a nominal solution (g^o, u^o, y^o) obtained by solving the DeePC (7) for an initial I/O trajectory (u^o_{ini}, y^o_{ini}) and reference trajectory r^o. For a new initial I/O trajectory (u_{ini}, y_{ini}) and reference trajectory r, the optimal solution is approximated by $u^* = u^o + \delta u$ using the DeeNE adaptation. The objective is now to develop a DeeNE framework for the data-driven optimal trajectory tracking problem. To that end, the DeeNE seeks to minimize the second-order variation of (9) subject to linearized constraints. More specifically, the DeeNE algorithm solves the following optimization problem with the given information δw_{ini} and δr as

$$\begin{aligned} \delta \mathbf{g}^* = \arg\min_{\delta \mathbf{g}} \; & J^{ne}_N \\ s.t. \quad & C^a_g \delta g = 0, \end{aligned} \tag{13}$$

where

$$J^{ne}_N = \delta^2 \bar{J}_N = \frac{1}{2} \begin{bmatrix} \delta w_{ini} \\ \delta g \\ \delta r \end{bmatrix}^T \begin{bmatrix} \bar{J}_{w_{ini}w_{ini}} & \bar{J}_{w_{ini}g} & \bar{J}_{w_{ini}r} \\ \bar{J}_{gw_{ini}} & \bar{J}_{gg} & \bar{J}_{gr} \\ \bar{J}_{rw_{ini}} & \bar{J}_{rg} & \bar{J}_{rr} \end{bmatrix} \begin{bmatrix} \delta w_{ini} \\ \delta g \\ \delta r \end{bmatrix}. \tag{14}$$

For (13), the augmented cost function are obtained as

$$\bar{J}^{ne}_N = \frac{1}{2} \begin{bmatrix} \delta w_{ini} \\ \delta g \\ \delta r \end{bmatrix}^T \begin{bmatrix} \bar{J}_{w_{ini}w_{ini}} & \bar{J}_{w_{ini}g} & \bar{J}_{w_{ini}r} \\ \bar{J}_{gw_{ini}} & \bar{J}_{gg} & \bar{J}_{gr} \\ \bar{J}_{rw_{ini}} & \bar{J}_{rg} & \bar{J}_{rr} \end{bmatrix} \begin{bmatrix} \delta w_{ini} \\ \delta g \\ \delta r \end{bmatrix} + \delta\mu^T C^a_g \delta g, \tag{15}$$

where $\delta\mu$ is the Lagrange multiplier.

By applying the KKT conditions to (15), one has

$$\bar{J}^{ne}_{\delta g} = 0, \qquad \delta\mu \geq 0. \tag{16}$$

where $\bar{J}^{ne}_{\delta g}$ indicates $\partial \bar{J}^{ne}_N / \partial \delta g$.

Theorem 1 (Data-Enabled Neighboring Extremal)**.** *Consider the optimization problem* (13)*, the augmented cost function* (15)*, and the KKT conditions* (16)*. If $\bar{J}_{gg} > 0$, then the DeeNE policy*

$$\begin{aligned} \delta g &= K^*_1 \delta w_{ini} + K^*_2 \delta r, \\ K^*_1 &= -\begin{bmatrix} I & 0 \end{bmatrix} K^o \begin{bmatrix} \bar{J}_{gw_{ini}} \\ 0 \end{bmatrix}, \\ K^*_2 &= -\begin{bmatrix} I & 0 \end{bmatrix} K^o \begin{bmatrix} \bar{J}_{gr} \\ 0 \end{bmatrix}, \\ K^o &= \begin{bmatrix} \bar{J}_{gg} & C^{aT}_g \\ C^a_g & 0 \end{bmatrix}^{-1} \end{aligned} \tag{17}$$

approximates the perturbed solution for the DeePC (7) *in the presence of initial I/O perturbation δw_{ini} and reference perturbation δr.*

Proof. Using (15) and the KKT conditions (16), one has

$$\bar{J}_{gw_{ini}} \delta w_{ini} + \bar{J}_{gg} \delta g + \bar{J}_{gr} \delta r + C^{aT}_g \delta\mu = 0. \tag{18}$$

Now, using (18) and the linearized safety constraints (13), one has

$$\begin{bmatrix} \bar{J}_{gg} & C^{aT}_g \\ C^a_g & 0 \end{bmatrix} \begin{bmatrix} \delta g \\ \delta\mu \end{bmatrix} = -\begin{bmatrix} \bar{J}_{gw_{ini}} \\ 0 \end{bmatrix} \delta w_{ini} - \begin{bmatrix} \bar{J}_{gr} \\ 0 \end{bmatrix} \delta r, \tag{19}$$

which yields

$$\begin{bmatrix} \delta g \\ \delta\mu \end{bmatrix} = -K^o \begin{bmatrix} \bar{J}_{gw_{ini}} \\ 0 \end{bmatrix} \delta w_{ini} - K^o \begin{bmatrix} \bar{J}_{gr} \\ 0 \end{bmatrix} \delta r. \tag{20}$$

Thus, the DeeNE policy (17) is obtained, and the proof is completed. □

Remark 1 (Singularity)**.** *$\bar{J}_{gg} > 0$ is essential for the DeeNE since it guarantees the convexity of* (13)*, and adding Assumption 1 makes a well defined K^o in* (17)*. If C^a_g is not full row rank, the matrix K^o will be singular, which leads to the failure of the proposed algorithm. This is addressed using the constraint back-propagation algorithm [28].*

Remark 2. *Using the control policy* (17)*, one can obtain $g^* = g^o + \delta g$, then $u^* = u^o + \delta u$ is obtained using $u = U_F g$. Therefore, one can conclude that $\delta u = K^r_{ne} \delta r + K^{ini}_{ne} \delta w_{ini}$.*

C. Nominal Non-Optimal Solution

The DeeNE is derived under the assumption that a nominal DeePC solution is available. In this subsection, we modify the DeeNE policy for a nominal non-optimal solution so that we can use the DeeNE solution as the nominal solution during the control process. For the nominal non-optimal sequences (w^o_{ini}, g^o, r^o), we assume that they satisfy the constraints described in (7) but may not satisfy the optimality condition $\bar{J}_g(w^o_{ini}, g^o, r^o, \mu^o) = 0$. Under this circumstance, the cost function (14) is modified as

$$J^{ne}_N = \delta^2 \bar{J}_N + \bar{J}^T_g \delta g = \frac{1}{2}\begin{bmatrix}\delta w_{ini}\\ \delta g\\ \delta r\end{bmatrix}^T \begin{bmatrix}\bar{J}_{w_{ini}w_{ini}} & \bar{J}_{w_{ini}g} & \bar{J}_{w_{ini}r}\\ \bar{J}_{gw_{ini}} & \bar{J}_{gg} & \bar{J}_{gr}\\ \bar{J}_{rw_{ini}} & \bar{J}_{rg} & \bar{J}_{rr}\end{bmatrix}\begin{bmatrix}\delta w_{ini}\\ \delta g\\ \delta r\end{bmatrix} + \bar{J}^T_g \delta g. \tag{21}$$

Considering the optimal control problem (13) and the cost function (21), the augmented cost function is modified as

$$\bar{J}^{ne}_N = \frac{1}{2}\begin{bmatrix}\delta w_{ini}\\ \delta g\\ \delta r\end{bmatrix}^T \begin{bmatrix}\bar{J}_{w_{ini}w_{ini}} & \bar{J}_{w_{ini}g} & \bar{J}_{w_{ini}r}\\ \bar{J}_{gw_{ini}} & \bar{J}_{gg} & \bar{J}_{gr}\\ \bar{J}_{rw_{ini}} & \bar{J}_{rg} & \bar{J}_{rr}\end{bmatrix}\begin{bmatrix}\delta w_{ini}\\ \delta g\\ \delta r\end{bmatrix} + \bar{J}^T_g \delta g + \delta\mu^T C^a_g \delta g. \tag{22}$$

Now, the following theorem is presented to modify the DeeNE policy for the nominal non-optimal solutions to the data-driven nonlinear optimal control problem.

Theorem 2 (Modified Data-Enabled Neighboring Extremal)**.** *Consider the optimization problem* (13)*, the KKT conditions* (16)*, and the augmented cost function* (22)*. If $\bar{J}_{gg} > 0$, then the DeeNE policy is modified for a nominal non-optimal solution as*

$$\begin{aligned}\delta g &= K^*_1 \delta w_{ini} + K^*_2 \delta r + K^*_3 \begin{bmatrix}\bar{J}_g\\ 0\end{bmatrix},\\ K^*_3 &= -\begin{bmatrix}I & 0\end{bmatrix} K^o,\end{aligned} \tag{23}$$

where the gain matrices K^*_1, K^*_2, and K^o are defined in (17)*.*

Proof. Using the KKT conditions (16) and the modified augmented cost function (22), one has

$$\bar{J}_{gw_{ini}} \delta w_{ini} + \bar{J}_{gg} \delta g + \bar{J}_{gr} \delta r + C^{aT}_g \delta\mu + \bar{J}_g = 0. \tag{24}$$

Now, using (24) and the linearized safety constraints (13), one has

$$\begin{bmatrix}\bar{J}_{gg} & C^{aT}_g\\ C^a_g & 0\end{bmatrix}\begin{bmatrix}\delta g\\ \delta\mu\end{bmatrix} = -\begin{bmatrix}\bar{J}_{gw_{ini}}\\ 0\end{bmatrix}\delta w_{ini} - \begin{bmatrix}\bar{J}_{gr}\\ 0\end{bmatrix}\delta r - \begin{bmatrix}\bar{J}_g\\ 0\end{bmatrix}, \tag{25}$$

which yields

$$\begin{bmatrix}\delta g\\ \delta\mu\end{bmatrix} = -K^o\begin{bmatrix}\bar{J}_{gw_{ini}}\\ 0\end{bmatrix}\delta w_{ini} - K^o\begin{bmatrix}\bar{J}_{gr}\\ 0\end{bmatrix}\delta r - K^o\begin{bmatrix}\bar{J}_g\\ 0\end{bmatrix}. \tag{26}$$

Thus, the modified DeeNE policy (23) is obtained, and the proof is completed. □

Remark 3 (Quadratic Cost)**.** *One can consider a quadratic cost function $J_N(\mathbf{y}, \mathbf{u}, \sigma_\mathbf{y}, \sigma_\mathbf{u}, \mathbf{g})$ as*

$$\begin{aligned}J_N(\mathbf{y}, \mathbf{u}, \sigma_\mathbf{y}, \sigma_\mathbf{u}, \mathbf{g}) = &\|y - r\|^2_Q + \|u\|^2_R\\ &+ \lambda_y\|\sigma_y\|^2_2 + \lambda_u\|\sigma_u\|^2_2 + \lambda_g\|g\|^2_2,\end{aligned} \tag{27}$$

where the positive semi-definite matrix $Q \in \mathbb{R}^{pN\times pN}$ and the positive definite matrix $R \in \mathbb{R}^{mN\times mN}$ are weighting matrices, and the positive parameters $\lambda_y, \lambda_u, \lambda_g \in \mathbb{R}$ are regularization weights. For the quadratic cost function (27)*, the DeePC is a quadratic program (QP) problem on the decision variable g, which requires an iterative solver, i.e. an online QP solver such as qpOASES [29]. To use the DeeNE, we have*

$$\begin{aligned}\bar{J}_g &= 2((Y_F g - r)^T Q Y_F + (U_F g)^T R U_F\\ &\quad + \lambda_y (Y_P g - y_{ini})^T Y_P + \lambda_u (U_P g - u_{ini})^T U_P + \lambda_g g^T),\\ \bar{J}_{gg} &= 2(Y^T_F Q Y_F + U^T_F R U_F + \lambda_y Y^T_P Y_P + \lambda_u U^T_P U_P + \lambda_g),\\ \bar{J}_{gw_{ini}} &= -2(\lambda_y Y^T_P + \lambda_u U^T_P),\\ \bar{J}_{gr} &= -2Y^T_F Q,\end{aligned} \tag{28}$$

where one can see that $\bar{J}_{gg} > 0$.

Algorithm 1 summarizes the DeeNE procedure for adapting a pre-computed nominal control solution to the small initial I/O and reference perturbations such that it achieves the optimal control using Theorem 2. When the nominal solution comes from the DeePC, Theorem 1 and Theorem 2 represent same control policy since we have $\bar{J}_g(w^o_{ini}, g^o, r^o, \mu^o) = 0$ for a nominal optimal solution. We use Theorem 2 for all time steps to employ the DeeNE solution as the nominal solution for the next time steps. It is worth noting that applying $u(k, k+1, \cdots, k+s) = u^*(0, 1, \cdots, s)$, $s \leq N-1$ to the plant reduces the computational cost, and in some cases may improve the control performance [12], [30]; however, Algorithm 1 represents $s = 0$ for the control framework.

Algorithm 1: Data-Enabled Neighboring Extremal

Parameter: U_P, Y_P, U_F, Y_F, C, Q, R, λ_y, λ_u, λ_g.
Input : w_{ini}, $r(0 : N-1)$.
Output : $\mathbf{u}(0 : T)$, $\mathbf{y}(0 : T)$.

```
for k = T_ini + 1 to T do
    if k == T_ini + 1 then
        Compute g*(0 : N − 1) using (7) and (27) ;
        u* = U_F g* ;
    end
    else
        Calculate μ^o using (12) ;
        Calculate K*_1, K*_2, K*_3 using (17) and (23) ;
        δw_ini = w_ini − w^o_ini;
        δr = r − r^o ;
        Calculate δg using (23) ;
        g* = g^o + δg;
        u* = U_F g* ;
    end
    Apply u(k) = u*(0) to the plant ;
    Measure y(k) from the plant ;
    g^o = g*;
    w^o_ini = w_ini;
    r^o = r ;
    w_ini = w(k − Tini + 1 : k) ;
    Update r(0 : N − 1) ;
end
```

IV. Simulation Results

In this part, we demonstrate the performance of the proposed DeeNE framework via a simulation example on a cart-inverted pendulum (see Fig. 1) whose system dynamics is described by:.

$$\begin{aligned}\ddot{z} &= \frac{F - K_d\dot{z} - m(L\dot{\theta}^2\sin(\theta) - g\sin(\theta)\cos(\theta)) - 2d_z}{M + m\sin^2(\theta)},\\ \ddot{\theta} &= \frac{\ddot{z}\cos(\theta) + g\sin(\theta)}{L} - \frac{d_\theta}{mL^2},\end{aligned} \tag{29}$$

where z and θ denote the position of the cart and the pendulum angle. $m = 1kg$, $M = 5kg$, and $L = 2m$ represent the mass of the pendulum, the mass of the cart, and the length of the pendulum. $g = 9.81m/s^2$ and $K_d = 10Ns/m$ are the gravity acceleration and the damping parameter. The variable force F controls the system under a friction force d_z and a friction torque d_θ. $T_s = 0.02s$ is considered as the sampling time for discretization of the model (29), and we assume d_z and d_θ as the process noises. The states, the outputs, the process noise, the measurement noise, and the control input constraint are expressed as

$$\begin{aligned} x &= [x_1, x_2, x_3, x_4]^T = [z, \dot{z}, \theta, \dot{\theta}]^T,\\ y &= [x_1, x_3]^T + v = [z, \theta]^T + v,\\ d &= [d_1, d_2, d_3, d_4]^T = [0, d_z, 0, d_\theta]^T,\\ &- 50 \le F \le 50. \end{aligned}$$

where d and v represent the process noise and measurement noise, respectively.

The following values are used for the simulation: $T_{ini} = 30$, $N = 45$, the simulation time $T = 200$, $x(0) = [0, 0, \pi/270, 0]^T$, and $d_z, d_\theta = 0.002(2rand(1, T) - 1)$. We generate the first initial trajectory (u_{ini}, y_{ini}) using zero control input, i.e. $u_{ini} = u(0 : 29) = 0$, which leads to the state $x(30) = [0.0151, 0.0783, 0.1225, 0.6200]^T$. Figs. 2 and 3 show the control performances of the DeeNE and the DeePC. For the DeePC, we use the DeePC policy (7), apply the length-s optimal control sequence to the plant, and update the initial trajectory w_{ini} for the next step (see Algorithm 2 in [12]). As we discussed in Algorithm 1, we use DeeNE policy (23) to avoid solving the DeePC problem at each step and reduce the computational cost. As is obvious from the Fig. 2, one can see that the DeeNE policy approximates the DeePC policy very well and is capable of adjusting the nominal DeePC by fully considering the initial I/O trajectory perturbations. From Fig. 3, one can see that the DeeNE achieves similar performance as compared to the DeePC; however, the DeeNE significantly reduces the computational cost of the DeePC as shown in Table II. Table I compares the cost-based performance and the computational time for the DeePC under various values of s, which demonstrates that we have the best performance for the considered system with $s = 5$. Table II illustrates the cost-based performance and the computational time for both DeePC and DeeNE under two cases $s = 0$ and $s = 5$, and one can see that the DeeNE with $s = 5$ shows the best performance for the regulation of the cart-inverted pendulum.

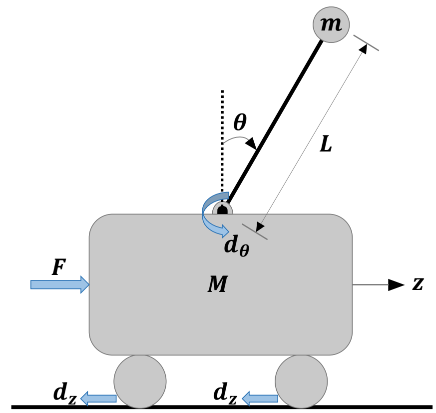

Fig. 1. Schematics of Cart-inverted pendulum.

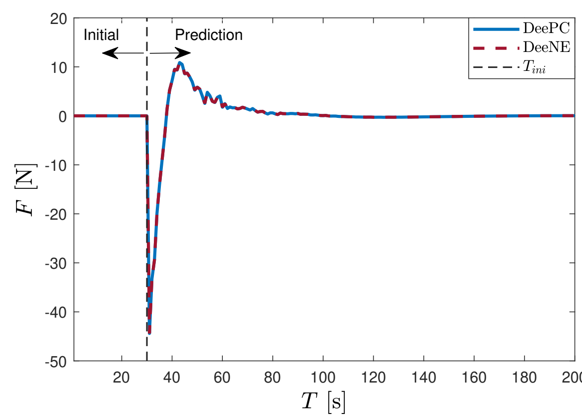

Fig. 2. Control input for cart-inverted pendulum.

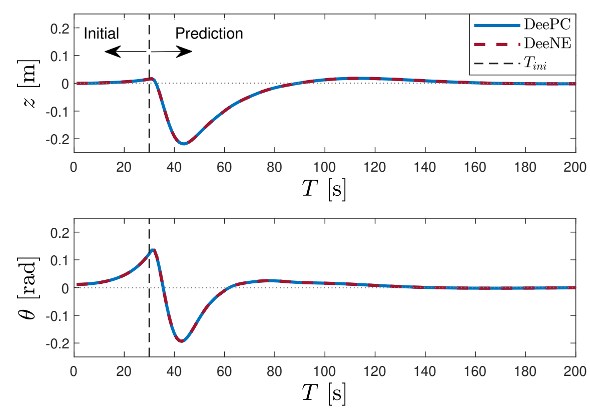

Fig. 3. System outputs for cart-inverted pendulum.

V. Conclusion

In this work, a computationally efficient data-driven optimal controller was studied for the nonlinear systems. Specifically, a DeeNE algorithm was developed to approximate the DeePC policy in the presence of input/output and reference trajectories perturbations. The developed DeeNE was based on the second-order variation of the original DeePC problem such that the computational load of the DeeNE grows linearly

TABLE I

Comparison of Performance and Computational Cost for the DeePC with various s.

DeePC	Cost	Time (per loop)
s = 0	22.3650	0.1419 ms
s = 5	22.1485	0.0284 ms
s = 10	22.7375	0.0159 ms

TABLE II

Comparison of Performance and Computational Cost for both DeePC and DeeNE

Controller	Cost	Time (per loop)
DeePC (s = 0)	22.3650	0.1419 ms
DeePC (s = 5)	22.1485	0.0284 ms
DeeNE (s = 0)	24.0375	0.0551 ms
DeeNE (s = 5)	23.5335	0.0102 ms

for the optimization horizon. This control approach alleviates the online computational burden and extends the applicability of data-driven optimal controllers. Simulations of the cart inverted pendulum system demonstrated the DeeNE's technological advances over the DeePC. Future work will involve the application of the DeeNE to complex, nonlinear, and networked real-world systems such as robots and connected vehicles.

References

[1] F. Lamnabhi-Lagarrigue, A. Annaswamy, S. Engell, A. Isaksson, P. Khargonekar, R. M. Murray, H. Nijmeijer, T. Samad, D. Tilbury, and P. Van den Hof, "Systems & control for the future of humanity, research agenda: Current and future roles, impact and grand challenges," *Annual Reviews in Control*, vol. 43, pp. 1–64, 2017.

[2] Z.-S. Hou and Z. Wang, "From model-based control to data-driven control: Survey, classification and perspective," *Information Sciences*, vol. 235, pp. 3–35, 2013.

[3] A. Vahidi-Moghaddam, M. Mazouchi, and H. Modares, "Memory-augmented system identification with finite-time convergence," *IEEE Control Systems Letters*, vol. 5, no. 2, pp. 571–576, 2020.

[4] A. Vahidi-Moghaddam, M. Mazouchi, and H. Modares, "Learning dynamics system models with prescribed-performance guarantees using experience-replay," in *2021 American Control Conference (ACC)*, pp. 1941–1946, IEEE, 2021.

[5] V. Breschi, A. Sassella, and S. Formentin, "On the design of regularized explicit predictive controllers from input-output data," *IEEE Transactions on Automatic Control*, 2022.

[6] A. Vahidi-Moghaddam, K. Chen, Z. Li, Y. Wang, and K. Wu, "Data-driven safe predictive control using spatial temporal filter-based function approximators," in *2022 American Control Conference (ACC)*, pp. 2803–2809, IEEE, 2022.

[7] A. Vahidi-Moghaddam, K. Chen, K. Zhang, Z. Li, Y. Wang, and K. Wu, "A unified framework for online data-driven predictive control with robust safety guarantees," *arXiv preprint arXiv:2306.17270*, 2023.

[8] J. Berberich, J. Köhler, M. A. Müller, and F. Allgöwer, "Data-driven model predictive control with stability and robustness guarantees," *IEEE Transactions on Automatic Control*, vol. 66, no. 4, pp. 1702–1717, 2020.

[9] C. De Persis and P. Tesi, "Formulas for data-driven control: Stabilization, optimality, and robustness," *IEEE Transactions on Automatic Control*, vol. 65, no. 3, pp. 909–924, 2019.

[10] J. C. Willems and J. W. Polderman, *Introduction to mathematical systems theory: a behavioral approach*, vol. 26. Springer Science & Business Media, 1997.

[11] J. C. Willems, P. Rapisarda, I. Markovsky, and B. L. De Moor, "A note on persistency of excitation," *Systems & Control Letters*, vol. 54, no. 4, pp. 325–329, 2005.

[12] J. Coulson, J. Lygeros, and F. Dörfler, "Data-enabled predictive control: In the shallows of the deepc," in *2019 18th European Control Conference (ECC)*, pp. 307–312, IEEE, 2019.

[13] P. G. Carlet, A. Favato, S. Bolognani, and F. Dörfler, "Data-driven continuous-set predictive current control for synchronous motor drives," *IEEE Transactions on Power Electronics*, vol. 37, no. 6, pp. 6637–6646, 2022.

[14] E. Elokda, J. Coulson, P. N. Beuchat, J. Lygeros, and F. Dörfler, "Data-enabled predictive control for quadcopters," *International Journal of Robust and Nonlinear Control*, vol. 31, no. 18, pp. 8916–8936, 2021.

[15] L. Huang, J. Coulson, J. Lygeros, and F. Dörfler, "Data-enabled predictive control for grid-connected power converters," in *2019 IEEE 58th Conference on Decision and Control (CDC)*, pp. 8130–8135, IEEE, 2019.

[16] W. Favoreel, B. De Moor, and M. Gevers, "Spc: Subspace predictive control," *IFAC Proceedings Volumes*, vol. 32, no. 2, pp. 4004–4009, 1999.

[17] K. Zhang, Y. Zheng, and Z. Li, "Dimension reduction for efficient data-enabled predictive control," *arXiv preprint arXiv:2211.03697*, 2022.

[18] A. Amiri-Margavi and H. Babaee, "On-the-fly reduced-order modeling of transient flow response subject to high-dimensional external forcing," *Bulletin of the American Physical Society*, 2022.

[19] Y. Zhong, A. Amiri-Margavi, H. Babaee, and K. Taira, "Optimally time-dependent mode analysis of vortex gust-airfoil wake interactions," *Bulletin of the American Physical Society*, 2022.

[20] R. Ghaemi, M. Abbaszadeh, and P. G. Bonanni, "Optimal flexibility control of large-scale distributed heterogeneous loads in the power grid," *IEEE Transactions on Control of Network Systems*, vol. 6, no. 3, pp. 1256–1268, 2019.

[21] A. Vahidi-Moghaddam, Z. Li, N. Li, K. Zhang, and Y. Wang, "Event-triggered cloud-based nonlinear model predictive control with neighboring extremal adaptations," in *2022 IEEE 61st Conference on Decision and Control (CDC)*, pp. 3724–3731, IEEE, 2022.

[22] A. Vahidi-Moghaddam, K. Zhang, Z. Li, X. Yin, Z. Song, and Y. Wang, "Extended neighboring extremal optimal control with state and preview perturbations," *arXiv preprint arXiv:2306.04830*, 2023.

[23] R. Ghaemi, S. Oh, and J. Sun, "Path following of a model ship using model predictive control with experimental verification," in *Proceedings of the 2010 American control conference*, pp. 5236–5241, IEEE, 2010.

[24] H. Park, J. Sun, S. Pekarek, P. Stone, D. Opila, R. Meyer, I. Kolmanovsky, and R. DeCarlo, "Real-time model predictive control for shipboard power management using the ipa-sqp approach," *IEEE Transactions on Control Systems Technology*, vol. 23, no. 6, pp. 2129–2143, 2015.

[25] Y. Xie, R. Ghaemi, J. Sun, and J. S. Freudenberg, "Model predictive control for a full bridge dc/dc converter," *IEEE Transactions on Control Systems Technology*, vol. 20, no. 1, pp. 164–172, 2011.

[26] H. Park, I. Kolmanovsky, and J. Sun, "Model predictive control of spacecraft relative motion maneuvers using the ipa-sqp approach," in *Dynamic Systems and Control Conference*, vol. 56123, p. V001T02A001, American Society of Mechanical Engineers, 2013.

[27] L. Huang, J. Zhen, J. Lygeros, and F. Dörfler, "Robust data-enabled predictive control: Tractable formulations and performance guarantees," *IEEE Transactions on Automatic Control*, vol. 68, no. 5, pp. 3163–3170, 2023.

[28] R. Ghaemi, J. Sun, and I. Kolmanovsky, "Neighboring extremal solution for discrete-time optimal control problems with state inequality constraints," in *2008 American Control Conference*, pp. 3823–3828, IEEE, 2008.

[29] F. Toso, P. G. Carlet, A. Favato, and S. Bolognani, "On-line continuous control set mpc for pmsm drives current loops at high sampling rate using qpoases," in *2019 IEEE Energy Conversion Congress and Exposition (ECCE)*, pp. 6615–6620, IEEE, 2019.

[30] L. Grüne, J. Pannek, M. Seehafer, and K. Worthmann, "Analysis of unconstrained nonlinear mpc schemes with time varying control horizon," *SIAM Journal on Control and Optimization*, vol. 48, no. 8, pp. 4938–4962, 2010.